Showcasing research from Dr. Shang Zhang's laboratory, R&D Department, Success Bio-Tech Co. Ltd., Jinan, China.

"PP-type" self-assembling peptides with superior rheological properties

Proline-terminated self-assembling peptides showed superior sol-gel transition ability compared to the classical self-assembling peptide RADA16. The rheological properties of self-assembling peptides are highly sequence dependent and the introduction of proline on the both ends of the peptide sequence not only enhances its sol-gel transition ability while also decreases the difficulties in synthesis and purification. These make "PP-type" self-assembling peptides an important candidate for further development of medical device products.

As featured in:

See Shang Zhang *et al.*, *Nanoscale Adv.*, 2021, **3**, 6056.

ROYAL SOCIETY OF CHEMISTRY

rsc.li/nanoscale-advances

Registered charity number: 207890

Nanoscale Advances

ROYAL SOCIETY OF CHEMISTRY

PAPER

View Article Online
View Journal | View Issue

Cite this: *Nanoscale Adv.*, 2021, **3**, 6056

"PP-type" self-assembling peptides with superior rheological properties†

Fangmin Li,[ab] Lichang Gao,[ab] Xudong Zhang,[ab] Pin Wang,[ab] Yuanxue Liu,[ab] Jinhui Feng,[ab] Chunxia Zhang,[ab] Chengru Zhao[ab] and Shang Zhang *[ab]

The ionic-complementary self-assembling peptides discovered by Zhang Shuguang have solution-to-gel (sol–gel) transition capacity and one such peptide RADA16 has been commercialized into hemostatic agents. However, their sol–gel transition ability was not obvious because the peptide aqueous solution with a concentration greater than 1% w/v appeared to be thick and viscous. The current report describes PP-type self-assembling peptides. In addition to the ionic-complementary sequence, they have prolines at both ends of the sequence. This feature has led to better solubility, lower viscosity of the peptide solution, and simplified synthesis and purification processes while maintaining the great gelling performance of the ionic-complementary peptides. The PP-type peptides self-assembled into a well-organized nanofiber scaffold as shown by TEM. Among the PP-type peptides, the PRVDP9 sequence peptide was tested as a hemostatic agent and a mucosal elevating agent. The results were comparable to the classic RADA16. The PP-type self-assembling peptides have superior sol–gel transition ability. Therefore, it is predicted that they will be more suitable to be transported through catheters or endoscopes and have higher commercialization potential as compared with the classic self-assembling peptide sequences.

Received 2nd July 2021
Accepted 1st September 2021

DOI: 10.1039/d1na00534k

rsc.li/nanoscale-advances

1. Introduction

The design of biomaterials mimicking the natural extracellular matrix (ECM) is greatly desired in biomaterial science to create suitable scaffolds for cell infiltration, proliferation, and tissue repair. The ionic-complementary self-assembling peptides are great ECM mimicking materials that have sol–gel transition capability.[1] They are completely composed of biologically natural component amino acids and are capable of self-assembling into supramolecular architectures from a solution phase to a solid phase. The self-assembly is accelerated by millimolar salt concentration under physiological pH conditions,[2,3] such as Na^+ or K^+, so the self-assembling peptide solution turns into a gel when it is exposed to physiological body fluids, including blood.[4–6] One such well-characterized peptide is RADA16, *i.e.*, AC-RADARADARADARADA-NH_2. A series of commercial products was designed using this sequence prepared at 2.5% w/v in pure water; for example, PuraStat® is used to stop bleeding during surgical operations including digestive tract operations,[7,8] PuraDerm Gel® is used for wound care, and PuraSinus® prevents bleeding and adhesions during sinus surgery. The ionic-complementary self-assembling peptide was firstly discovered by Zhang Shuguang in the yeast protein zuotin in 1993.[9,10] The sequence typically comprises alternating positively charged, hydrophobic, and negatively charged amino acids.[11] The peptides form a checkerboard-like stable structure through ionic complementary forces,[2,3] then assemble into a typical ß-sheet structure and finally become a nanofiber network hydrogel under triggering conditions such as contact with electrolytes or a change in the osmotic pressure.[12–14]

Numerous studies have been performed on self-assembling peptides. The application of self-assembling peptide solution has prevented liver hemorrhage and promoted liver tissue regeneration,[15] prevented bleeding at the vascular grafting site,[16] reduced blood loss in the kidney surgery,[6,17,18] prevented bleeding of the digestive tract in the endoscopic submucosal dissection (ESD), endoscopic mucosal resection (EMR) surgery and in the management of gastrointestinal bleeding.[19,20] It achieved rapid healing of the mucosa[21,22] and achieved hemostasis and accelerated osteosis as compared with bone wax.[23] Self-assembled peptides were also researched as drug-releasing vehicles and cellular scaffolds.[24,25] They were used to regenerate liver,[26,27] neurons,[28,29] cartilage,[30–33] and for angiogenesis.[34,35] In addition, self-assembling peptides have been applied in the joint cavity for lubrication and the prevention of tissue adhesion.[36]

[a]*Success Bio-Tech Co., Ltd., 2222 Kaituo Road, Jinan, 250101, China. E-mail: shang.zhang@succcessbio-tech.com*

[b]*Biomedical Material Engineering Laboratory of Shandong Province, 2222 Kaituo Road, Jinan, 250101, China*

† Electronic supplementary information (ESI) available. See DOI: 10.1039/d1na00534k

The application potential of the self-assembling peptides is huge.[37] However, currently, there are very few commercialized products due to the high dose and high cost in some application scenarios. To successfully design a self-assembling peptide commercial product, various aspects need to be considered, including solubility, storage conditions, production, purification yield, and viscosity. The sol–gel transition ability of the classic RADA16 peptide was not that obvious and the peptide aqueous solution with a concentration greater than 1% w/v appeared to be thick and viscous.

The current report describes PP-type self-assembling peptides. Compared with the commercialized RADA16 peptide, the novel peptides have proline amino acids at both N- and C-ends, in addition to the ionic complementary sequence (Table 4), and have the features of high solubility, low solution viscosity, low manufacturing cost, and low purification cost. Among the PP-type peptides, the PRVDP9 sequence peptide, AC-PRVDVRVDP-NH_2, was tested as a hemostatic agent and a mucosal elevating agent. The results were comparable to the classic RADA16. PP-type self-assembling peptides have superior sol–gel transition ability as compared to RADA16, which in this article specifically means that the PP-type self-assembling peptides have better flowability before gel formation and equivalent gel strength after gel formation. Therefore, it is predicted that they will be more suitable to be transported through catheters or endoscopes and have higher commercialization potential, especially for interventional therapies and endoscopic therapies.

2. Experimental section

2.1. Peptide synthesis and purification

The peptides in this report were synthesized using the fluorenylmethoxycarbonyl protecting group (FMOC) solid-phase synthesis and purified by HPLC.[38,39] The peptides were then lyophilized, having a purity of more than 95%. After identification by TOF-MS, they were used for subsequent experiments.

2.2. Circular dichroism (CD) spectra

The PRVDP9 peptides were prepared in MILLI-Q water with concentrations of 5 μM, 10 μM, 20 μM, 50 μM, 100 μM, 200 μM, filtered and tested with a CD (MOS-500 Spectrometer). The average residue molar ellipticity $[\theta]$ was used to estimate the secondary structure of the peptides. The formula used for the calculation was $[\theta] = \theta/10lcMn$ (where θ is the measured value minus the blank, l is the optical path length of the cuvette with a unit of cm, cM is the concentration with a unit of mol L^{-1} and n is the number of amino acid residues). The $[\theta]$ value was used to plot against the wavelength.

2.3. Preparation of peptide hydrogel

Here 1%, 2%, and 3% w/v PRVDP9 solutions were prepared in pure water in a vial. 10× PBS was calculated and added so that the final concentration of PBS in the system does not exceed 1×. This was allowed to stand for 10 seconds and the vial was turned upside down.

2.4. Transmission electron microscope (TEM)

The PRVDP9 solution prepared in pure water with a concentration of 6 mg ml^{-1} was added to 10× PBS to make the PBS concentration in the system not exceed 1×. The resulting peptide hydrogel was dropped on the copper mesh. The excessive hydrogel was removed with a filter paper. The hydrogel was stained with 1% phosphotungstic acid for 15 seconds, then air-dried. The images were taken with a TEM (JEOL JEM).

2.5. Rheological properties

To measure the storage modulus of the peptide gel, the following experiments were performed. Peptide solutions were prepared as described in Table 1. Here, 10× PBS was calculated and added to make the PBS concentration in the system not exceed 1×. No less than 2 ml of hydrogel was added slowly to the center of the rheometer plate (Kinexus Ultra+). The gap was 450 μm between the plates. The sample was kept at 37 °C for 5 minutes under a shear stress of 1 Pa. Frequency sweeps ranging from 0.1 Hz to 10 Hz were performed. The storage modulus was recorded at a frequency of 1 Hz.

To measure the viscosity, peptide solutions were prepared as described in Tables 2 and 4. Here, 2 ml of peptide solution was added slowly to the center of the rheometer plate (RS.SST Brookfield). The gap between the plates was 1 mm. Shear rates ranging from 1 to 1000 s^{-1} were performed.

2.6. Liver hemostasis

The rabbit (New Zealand white male rabbits, 2–4 kg, Xilingjiao Animal Breeding Center, Jinan, China) liver hemorrhaging model was used to evaluate the *in vivo* hemostatic ability of peptides. All animal procedures and animal care were performed in accordance with the Shandong Laboratory Animal Regulations. All animal procedures were approved by the Animal Welfare and Ethics Committee of Success Bio-Tech Co. Ltd.

The peptide PRVDP9 was prepared at a concentration of 3% w/v or 4% w/v in water. RADA16 was prepared at 2.5% w/v. The rabbits were anesthetized by the intravenous administration of 2% w/v pentobarbital sodium. The abdominal cavity was opened to expose the liver. Incisions were made 1 cm long and 3 mm deep using a scalpel. The blood was gently removed with

Table 1 Peptide samples for rheological property testing

Sequence ID	Sequence	Concentrations
RADA16	AC-RADARADARADARADA-NH_2	1%, 2%, 2.5%
RADA12	AC-RADARADARADA-NH_2	1%, 2%
RADA8	AC-RADARADA-NH_2	1%, 2%
RVDV8	AC-RVDVRVDV-NH_2	1%, 2%
VRVDV9	AC-VRVDVRVDV-NH_2	1%, 2%
PRVD9	AC-PRVDVRVDV-NH_2	1%, 2%, 3%, 4%
PRVDP9	AC-PRVDVRVDP-NH_2	1%, 2%
PRVD17	AC-PRVRVRVDPRVDVRVDP-NH_2	1%, 2%
RVDP8	AC-RVDVRVDP-NH_2	1%, 2%
PKVEP9	AC-PKVEVRVDP-NH_2	1%, 2%, 3%, 4%

Table 2 Viscosity of the self-assembled peptides with different sequences[a]

Sequence ID	Concentration (w/v)	Viscosity (Pa s)
RVDV8	1%	457.64 ± 20.86***
	2%	1684.31 ± 43.27***
VRVDV9	1%	625.6 ± 40.25***
	2%	2048.28 ± 204.5**
PRVDP9	3%	Under the detection limit
	4%	Under the detection limit
PKVEP9	3%	Under the detection limit
	4%	Under the detection limit
PRVD9	1%	658.25 ± 26.4***
	2%	1546.21 ± 49.5***
PRVD17	1%	1254.18 ± 31.25***
	2%	3576.76 ± 86.14***
RADA16	1%	955.17 ± 46.7
	2%	1817.96 ± 57.6
	2.5%	2514.57 ± 68.1

[a] Data represent mean ± SD and $n = 3$ for each group. **$P < 0.01$, ***$P < 0.001$. One-way ANOVA with Tukey's *post hoc* test was used for the calculation. Data in the RADA16 group were used as the control for comparison.

gauze. The peptide solution was immediately applied at the wound site with a syringe. The bleeding time was recorded.

2.7. Mucosal elevation

The rabbits were anesthetized by the intravenous administration of 2% w/v pentobarbital sodium, then laparotomized by median incision. An incision was made in the stomach to expose the gastric mucosa. Either 0.5 ml of 1% w/v PRVDP9 peptide solution, saline, or 10 mg ml^{-1} of sodium hyaluronate (Fruida, Jinan, China) was injected into the gastric submucosal layer with a syringe and a 25 G needle. For the colon mucosal elevation, an incision was made to expose the colon mucosa. Either 0.5 ml of 1% w/v PRVDP9 peptide solution, saline, or 10 mg ml^{-1} of sodium hyaluronate (Fruida, Jinan, China) was injected into the colon submucosal layer with a syringe and a 25 G needle. After 30 min of surveillance, the animals were sacrificed. The tissue samples were prepared by fixation with 4% v/v formaldehyde for 2 days, embedded with paraffin, sliced, and processed with hematoxylin–eosin (HE) staining.

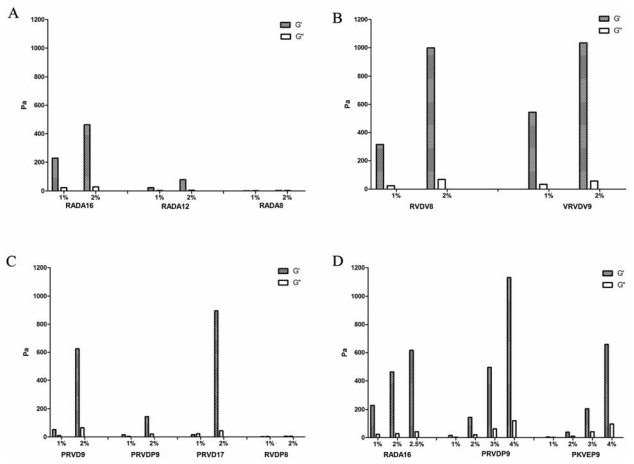

Fig. 1 Storage modulus of self-assembling peptides with different sequences. (A) The longer RADA repeats resulted in the higher storage modulus of the peptide gel. (B) The storage modulus of RVDV8 VRVDV9 containing Val instead of Ala. The storage modulus value of RVDV8 is higher than RADA8 (A) which contains the same number of repeats. (C) The storage modulus of the peptide gel was related to the position of Pro within the sequences. (D) PRVDP9 can be prepared with a high concentration to increase the resulting gel strength because of its high solubility.

3. Results

3.1. The screening of self-assembling peptides with better solubility and a shorter sequence

The formation of the self-assembling peptide gel and its mechanical properties are influenced by several factors, including the amino acid sequence, the level of hydrophobicity, and the length of the peptides.[1] The formation of the self-assembling peptide gel was often measured by the storage modulus of the resulting gel. The classic ionic-complementary self-assembling peptide RADA16 sequence consists of 16 amino acids. The shorter the peptide sequence, the lower the R&D and production cost will be. However, if the length of RADA repeats was reduced, the gel-forming capacity and the

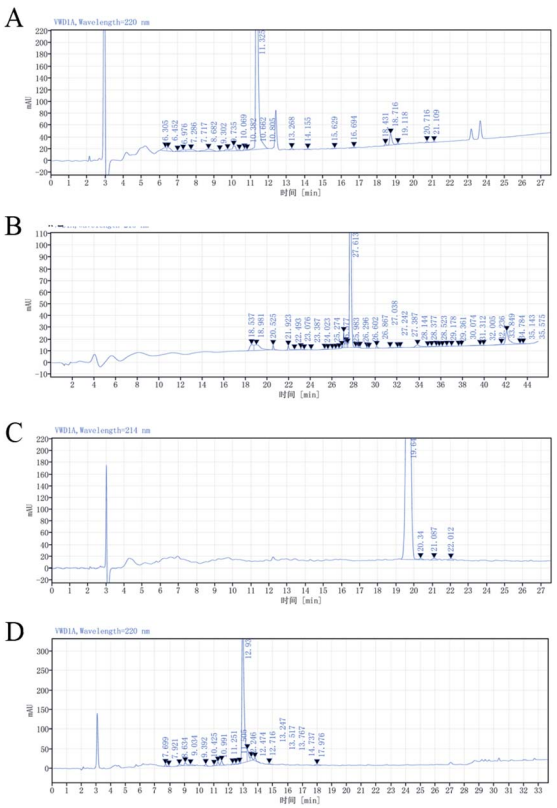

Fig. 2 Peptide synthesis and purification. HPLC analysis of the crude peptide with the following sequence IDs: RVDV8 (A), VRVDV9 (B), PRVDP9 (C), RADA16 (D), synthesized by the Fmoc solid-phase synthesis method. The graphs are representative data.

Table 3 The purity and yield of self-assembling peptides with different sequences

Sequence ID	Purity	Yield of crude peptide
RVDV8	82.74%	40.38%
VRVDV9	69.75%	31.57%
PRVDP9	97.68%	69.12%
RADA16	80.20%	49.56%

mechanical properties of the resulting gel would decrease, as indicated by the storage modulus of the peptide gel (Fig. 1A). Not surprisingly, RADA8 did not show any self-assembling compacity. To reduce the production cost, we tried to use Val to replace Ala in the classic sequence of RADA because theoretically using more hydrophobic amino acids within the sequence can increase the mechanical properties of the peptide gel.[40,41] RVDV8 and VRVDV9 showed great gel-forming capacity; the storage moduli of the resulting gels were similar or even higher than RADA16 at the same peptide concentration (Fig. 1A and B). The viscosity of the RVDV8 or VRVDV9 solution prepared in pure water was comparable to the RADA16 solution (Table 2). They were all considerably viscous at more than 1% w/v. The solubilities of RVDV8, VRVDV9, and RADA16 in pure water were less than 3% w/v at room temperature. The low solubility led to difficulty in the production and purification. The resulting crude peptides generated from the solid-phase synthesis of the RVDV8, RVDV8 and RADA16 purities of 82.74% w/v, 69.75% w/v, and 80.20% w/v respectively, as shown by HPLC analysis (Fig. 2A, B, and D). Because of their low solubility at room temperature, the yields of VRVDV9 and RVDV8 after the purification process were 31.57% w/v and 40.38% w/v, respectively (Table 3). Although VRVDV9 and RVDV8 had shorter sequences, their production costs and yields were not suitable due to their low solubility in pure water.

It has been reported the pyrrole ring of the side chain of Pro is conducive to the formation of the secondary structure of random coils, which was further considered to increase the solubility of the peptide and prevent the entanglement between the peptide chains.[42] "PP-type" peptides were designed. In addition to the classic ionic-complementary sequence, they have an additional Pro at both N- and C-ends of the sequence. We also tested the ionic-complementary peptide with only one additional Pro at either the N- or C-end. PRVDP9 showed superior solubility as compared with PRVD9, although both have gel-forming capacity (Fig. 1C, Table 2). The viscosity of the PRVDP9 peptide solution was similar to that of the water solvent, even at 4% w/v (Table 2). The crude peptide purity and the purification yield were reasonably high, up to 97.68% w/v (Fig. 2C, Table 3). The PP-type peptides showed great commercialization potential.

Next, we screened the PP-type peptides with different sequences as shown in Table 4, the results showed that only PRVDP9 and PKVEP9 had good gel-forming capacities. The solubilities of PRVDP9 and PKVEP9 were as high as 4% w/v in pure water at room temperature and the viscosities of the above peptide solutions were under the detection limit (Table 2). In comparison, RADA16 self-assembled into a gel when the concentration of the peptide solution was at 3% w/v. The viscosity of the RADA16 solution, as low as 1% w/v, was 955.17 ± 46.7 Pa s. Since the commercial products used 2.5% w/v as the final concentration, we used 2.5% w/v RADA16 for most of the experiments. The storage modulus of 4% w/v PRVDP9 was more than 1130 Pa, as compared with the 616.4 Pa of 2.5% w/v RADA16 and 658.3 Pa of 4% w/v PKVEP9 (Fig. 1D). The PP-type peptides had more obvious sol–gel transition performances.

3.2. PRVDP9 secondary structure and tertiary structure

The CD spectra of PRVDP9 showed that there was no typical secondary structure at each concentration although they were similar to the ß-sheet spectra at 10 μM and 20 μM concentrations, probably affected by the additional amino acids Pro (Fig. 3). The PRVDP9 peptide showed good gel-forming ability when mixed with PBS (Fig. 4C). TEM showed that the PRVDP9 peptide formed a dense nanofiber scaffold (Fig. 4A and B).

3.3. Liver hemostasis

The PP-type peptide PRVDP9 was compared with RADA16 to evaluate its hemostatic performance. The PRVDP9 peptide

Table 4 The sol–gel performance of PP-type self-assembling peptides[a]

Sequence	Conc. (w/v)	Soluble or not at R.T.	Viscosity (Pa s)	Gel forming
AC-PRVDVRVDP-amide (PRVDP9)	1%	Yes	Under the detection limit	Yes
	2%	Yes	Under the detection limit	Yes
AC-PKVEVKVEP-amide (PKVEP9)	1%	Yes	Under the detection limit	Yes
	2%	Yes	Under the detection limit	Yes
AC-PRIDIRIDP-amide (PRIDP9)	1%	Yes	543.25 ± 19.46***	No
	2%	Yes	1246.25 ± 26.45***	No
AC-PKIEIKIEP-amide (PKIEP9)	0.5%	Yes	1035.84 ± 31.68***	No
	1%	Yes	3565.64 ± 157.36***	No
AC-PKLDLKLDP-amide (PKLDP9)	1%	Yes	Under the detection limit	No
	2%	Yes	Under the detection limit	No
Ac-PRVEVRVEP-amide (PRVEP9)	0.5%	No	—	—
	1%	No	—	—

[a] Data represent mean ± SD and $n = 3$ for each group. ***$P < 0.001$. Two tailed t-tests were used for the calculation.

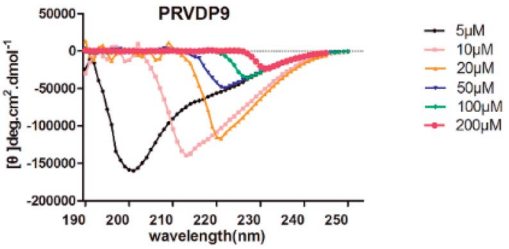

Fig. 3 CD spectra of peptide PRVDP9. CD spectra of peptide PRVDP9 at various concentrations (5 μM, 10 μM, 20 μM, 50 μM, 100 μM, 200 μM).

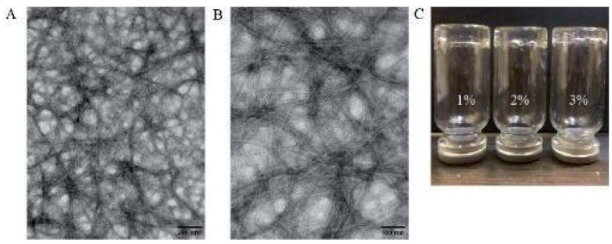

Fig. 4 TEM images of peptide PRVDP9. (A and B) TEM images of 6 mg ml^{-1} peptide PRVDP9 at different magnifications. (C) Peptide hydrogel (1%, 2%, 3%) formed in the vial.

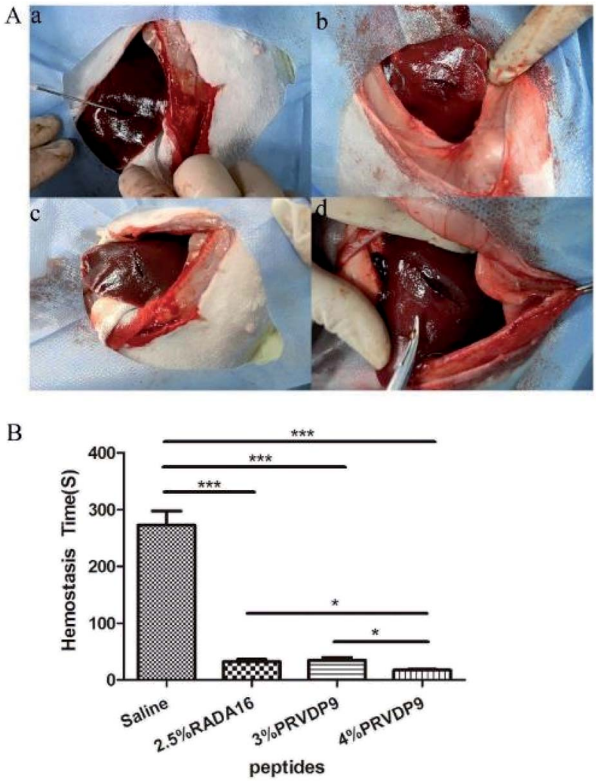

Fig. 5 Testing of the self-assembling peptides as hemostatic agents *in vivo*. (A) The rabbit liver hemostasis model *in vivo* (A, a). Peptides were applied to the wound site with a 1 ml syringe. The 2.5% RADA16 (A, b), 3% PRVDP9 (A, c), and 4% PRVDP9 (A, d) stopped liver bleeding within 1 minute. (B) Hemostasis time of different peptides in the liver hemostasis model. Data represent mean ± SD and $n = 3$ for each group. *$P < 0.05$, ***$P < 0.001$. One-way ANOVA with Tukey's post hoc test was used for the calculations.

solution quickly formed a gel as soon as it came in contact with the blood after its application to the wound site. Peptides including 2.5% RADA16, 3% PRVDP9 and 4% PRVDP9 achieved hemostasis within 1 minute (Fig. 5A). After 2 minutes of application, the excess gel was removed, the wound site was visible, and there was no more blood exudation (Fig. 5A). Compared to saline, the hemostasis times of the peptide solution groups were significantly reduced and there was no significant difference between the 2.5% RADA16 and 3% PRVDP9 group (Fig. 5B). It was noted that 4% PRVDP9 exhibited better hemostatic capacity than 2.5% RADA16 and 3% PRVDP9 (Fig. 5B).

3.4. PRVDP9 mucosal elevation

Considering the great rheological properties and adequate gel strength of the peptide PRVDP9, we believe that its solution could be used as a mucosal elevating agent for EMR and ESD surgery, and so we compared it with normal saline and the widely used sodium hyaluronate. We injected the above agents into the gastric or colon submucosal layer using a syringe with a 25 G needle. From the aspect of ease of use, sodium hyaluronate is difficult to push during injection because of its viscous nature, which leads to difficulty in controlling the plunging forces and the consequent injection volumes. The histology results showed that the sodium hyaluronate dissipated and the liquid cushion collapsed. The normal saline and the PRVDP9 solution were comparatively easier to push during the injection procedure. However, the saline flew out during the injection process and no obvious bulge was observed after the injection. In contrast, following the injection of PRVDP9, there was an obvious bulge in the mucosa and there was no outflowing fluid during the injection and the sampling. HE staining showed that the mucosa and submucosa of the colonic tissue injected with saline were separated, but the mucosa did not bulge (Fig. 6A). HE staining showed a small amount of blue-stained sodium hyaluronate and a large cavity appeared under the mucosa following the injection with sodium hyaluronate, suggesting that sodium hyaluronate did not play a long-lasting supporting role (Fig. 6A). The colonic mucosa injected with PRVDP9

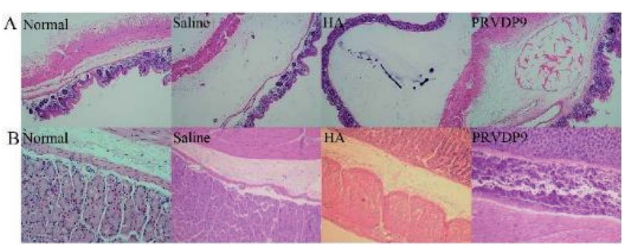

Fig. 6 PRVDP9 solution as a mucosal elevating agent. (A) HE staining of colonic mucosa filled with normal saline, sodium hyaluronate, or PRVDP9. (B) HE staining of gastric mucosa filled with normal saline, sodium hyaluronate, and PRVDP9.

showed a bulge, and the cavity was evenly filled with red-stained self-assembling peptides (Fig. 6A). The experiments for the gastric mucosal showed similar results (Fig. 6B). Multiple injections of the sodium hyaluronate solution are usually required to maintain a continuous separation of the mucosa from the submucosa in clinical practices. In contrast, the PRVDP9 solution was able to quickly turn into a gel after being injected submucosally. It is predicted that the resulting transparent solid hydrogel cushion will not be affected by surgical procedures, which will greatly reduce the difficulty of surgical operations and simplify the surgical procedures. As such, the PRVDP9 solution is expected to be a new generation of submucosal injection.

4 Discussion

The design of a biomaterial mimicking natural ECM is greatly desired in biomaterial science, regenerative medicine, and medical devices. The ionic-complementary self-assembling peptides have such ECM-mimicking features because they are made of pure amino acids and have the sol–gel transition function. The classic sequence RADA16 has been used to develop a series of medical device products such as hemostatic agents and anti-adhesive devices. However, the sol–gel transformation is not great because once the concentration of RADA16 was greater than 1% w/v, the solution self-assembled and became viscous and thick. Here, we developed PP-type self-assembling peptides that have superior sol–gel transition ability as compared with RADA16.

The classic RADA16 has 16 amino acids, consisting of 50% hydrophobic amino acids, and alternating acidic and basic amino acids. The long length and the self-assembling nature made synthesis and purification difficult. To make the peptide length shorter, more hydrophobic amino acids are needed within the sequence. However, although RVDV8 and VRVDV9 have shorter sequences, their production was still very difficult because of the low solubility. We found that the additional Pro at both ends of the ionic-complementary sequence helped to increase the solubility and maintained the self-assembling nature of the peptides in certain situations. PRVDP9 and PKVEP9 are highly soluble peptides and maintained great potential for gel formation. It was much easier to produce PRVDP9 and PKVEP9 peptides with very high crude peptide purity and high final yield. It is speculated that the introduction of proline weakened the ß-sheet structure of the self-assembling peptide, consequently preventing the entanglement between peptide chains and facilitating the synthesis. CD spectral results provided evidence in support of the speculations. It is well known that ionic-complementary self-assembling peptides exhibit typical ß-sheet secondary structures, but the PRVDP9 peptide no longer exhibited the typical ß-sheet structures in solution and the varied secondary structure did not diminish the gel-forming capacity. The 1–3% w/v RVD9 peptide solution quickly self-assembled into a gel upon contact with the PBS solution. The peptides self-assembled into a well-organized nanofiber scaffold as shown by TEM. The density of the nanofiber scaffold can be enforced by increasing the concentration of the peptide solution, which provides the possibility to meet different application scenarios.

RADA16 is often used at a concentration from 1% to 2.5% w/v according to different indications. We found that 1% w/v RADA16 solution had a considerable viscosity and a 2.5% w/v product had rather poor fluidity, which might not be suitable for delivery through catheters and endoscopes during interventional therapies and endoscopic therapies.

The viscosity of the PRVDP9 solution was extremely low, even when the concentration was as high as 4% w/v. The storage modulus of the gel formed by 3% w/v PRVDP9 was almost equivalent to that of 2.5% w/v RADA, while the gel formed by 4% w/v PRVDP9 had a higher gel strength. The data showed that a product with better sol–gel transition capacity could be designed using PP-type peptides, especially PRVDP9.

The hemostasis times of a rabbit liver hemostasis model treated with 3% w/v PRVDP9 or 2.5% w/v RADA16 solution were equivalent, while the treatment with 4% w/v PRVDP9 resulted in a shorter hemostasis time. The hemostatic performance was correlated with the mechanical data of the peptide gel. It was apparent that the better solubility of PRVDP9 helped the spreading of the peptide solution at the wound site and improved the hemostasis.

We tried to use an animal model to study the potential of the peptides as a mucosal elevating agent for EMR and ESD surgery. The low viscosity made PRVDP9 very easy to push during the injection procedure. After PRVDP9 solution was delivered into the submucosal gap, a solid peptide gel formed immediately and maintained the mucosal bulge for a long time, which indicated the great functional performance as a mucosal elevating agent. HE staining showed that the hydrogel accumulated with an even and dense distribution as a spacer between the mucosal and submucosal tissues.

5 Conclusion

PP-type self-assembling peptides have superior sol–gel transition ability and are easy to manufacture. It is predicted that they will be more suitable to be transported through catheters or endoscopes and have greater commercialization potential as compared with classic self-assembling peptide sequences.

Conflicts of interest

The authors are working in Success Bio-tech Co., Ltd. Jinan, 250101, China, which is a medical device provider.

Acknowledgements

The authors thank for the research funding support from Major Science and Technology Innovation Projects of Shandong Province (2019JZZY011107).

References

1 S. Zhang, *Interface Focus*, 2017, 7, 20170028.

2 S. Zhang, T. Holmes, C. Lockshin and A. Rich, *Proc. Natl. Acad. Sci. U. S. A.*, 1993, **90**, 3334–3338.
3 S. Zhang, C. Lockshin, R. Cook and A. Rich, *Biopolymers*, 1994, **34**, 663–672.
4 S. Subramaniam, K. Kandiah, S. Thayalasekaran, G. Longcroft-Wheaton and P. Bhandari, *United Eur. Gastroenterol. J.*, 2019, **7**, 155–162.
5 R. G. Ellis-Behnke, Y.-X. Liang, D. K. C. Tay, P. W. F. Kau, G. E. Schneider, S. Zhang, W. Wu and K.-F. So, *Nanomedicine*, 2006, **2**, 207–215.
6 G. de Nucci, R. Reati, I. Arena, C. Bezzio, M. Devani, C. D. Corte, D. Morganti, E. D. Mandelli, B. Omazzi, D. Redaelli, S. Saibeni, M. Dinelli and G. Manes, *Endoscopy*, 2020, **52**, 773–779.
7 M. Ortenzi and A. Haji, *Minim Invasive Ther. Allied Technol.*, 2020, 1–6.
8 S. Subramaniam, K. Kandiah, S. Thayalasekaran, G. Longcroft-Wheaton and P. Bhandari, *United Eur. Gastroenterol. J.*, 2018, **7**, 155–162.
9 S. Zhang, C. Lockshin, A. Herbert, E. Winter and A. Rich, *EMBO J.*, 1992, **11**, 3787–3796.
10 S. Zhang, T. Holmest, C. Lockshin and A. Rich, *Proc. Natl. Acad. Sci. U. S. A.*, 1993, **90**, 3334–3338.
11 X. Wu, L. He, W. Li, H. Li, W.-M. Wong, S. Ramakrishna and W. Wu, *Regener. Biomater.*, 2017, **4**, 21–30.
12 X. Zhao, F. Pan, H. Xu, M. Yaseen, H. Shan, C. A. Hauser, S. Zhang and J. R. Lu, *Chem. Soc. Rev.*, 2010, **39**, 3480–3498.
13 F. Gelain, A. Horii and S. Zhang, *Macromol. Biosci.*, 2007, **7**, 544–551.
14 A. R. Cormier, X. Pang, M. I. Zimmerman, H. X. Zhou and A. K. Paravastu, *ACS Nano*, 2013, **7**, 7562–7572.
15 T.-Y. Cheng, H.-C. Wu, M.-Y. Huang, W.-H. Chang, C.-H. Lee and T.-W. Wang, *Nanoscale*, 2013, **5**, 2734.
16 H. Masuhara, T. Fujii, Y. Watanabe, N. Koyama and K. Tokuhiro, *Ann.Thorac. Cardiovasc. Surg.*, 2012, **18**, 444–451.
17 H. Song, L. Zhang and X. Zhao, *Macromol. Biosci.*, 2010, **10**, 33–39.
18 M. Morshuis, M. Schönbrodt and J. Gummert, *J. Heart Lung Transplant.*, 2019, **38**, S194.
19 S. Subramaniam, K. Kandiah, F. Chedgy, C. Fogg, S. Thayalasekaran, A. Alkandari, M. Baker-Moffatt, J. Dash, M. Lyons-Amos, G. Longcroft-Wheaton, J. Brown and P. Bhandari, *Endoscopy*, 2021, **53**, 27–35.
20 M. Pioche, M. Camus, J. Rivory, S. Leblanc, I. Lienhart, M. Barret, S. Chaussade, J.-C. Saurin, F. Prat and T. Ponchon, *Endosc. Int. Open*, 2016, **04**, E415–E419.
21 M. Gagliardi, M. Sica, G. Oliviero, A. Maurano and C. Zulli, *J. Gastrointest. Liver Dis.*, 2021, DOI: 10.15403/JGLD-3680, https://www.jgld.ro/jgld/index.php/jgld/article/view/3680.
22 M. Ortenzi and A. Haji, *Minim. Invasive Ther. Allied Technol.*, 2020, 1–6.
23 M. Wu, Z. Ye, H. Zhu and X. Zhao, *Biomacromolecules*, 2015, **16**, 3112–3118.
24 M. L. Briuglia, A. J. Urquhart and D. A. Lamprou, *Int. J. Pharm.*, 2014, **474**, 103–111.
25 Y. Nagai, L. D. Unsworth, S. Koutsopoulos and S. Zhang, *J. Contr. Release*, 2006, **115**, 18–25.
26 C. E. Semino, J. R. Merok, G. G. Crane, G. Panagiotakos and S. Zhang, *Differentiation*, 2003, **71**, 262–270.
27 Y. Kumada and S. Zhang, *PloS one*, 2010, **5**, e10305.
28 T. C. Holmes, S. de Lacalle, X. Su, G. Liu, A. Rich and S. Zhang, *Proc. Natl. Acad. Sci. U. S. A.*, 2000, **97**, 6728–6733.
29 J. Guo, K. K. Leung, H. Su, Q. Yuan, L. Wang, T. H. Chu, W. Zhang, J. K. Pu, G. K. Ng, W. M. Wong, X. Dai and W. Wu, *Nanomedicine*, 2009, **5**, 345–351.
30 A. Mujeeb, A. F. Miller, A. Saiani and J. E. Gough, *Acta Biomater.*, 2013, **9**, 4609–4617.
31 L. Li, J. Li, J. Guo, H. Zhang, X. Zhang, C. Yin, L. Wang, Y. Zhu and Q. Yao, *Adv. Funct. Mater.*, 2019, **29**, 1807356.
32 F. Gelain and Z. Luo, *Chem. Rev.*, 2020, **120**, 13434–13460.
33 R. Wang, Z. Wang, Y. Guo, H. Li and Z. Chen, *J. Biomater. Sci., Polym. Ed.*, 2019, **30**, 713–736.
34 C. Han and Z. Zhang, *Int. J. Nanomed.*, 2020, **15**, 10257–10269.
35 H. D. Guo, G. H. Cui, J. J. Yang, C. Wang, J. Zhu, L. S. Zhang, J. Jiang and S. J. Shao, *Biochem. Biophys. Res. Commun.*, 2012, **424**, 105–111.
36 C. J. Bell, L. M. Carrick, J. Katta, Z. Jin, E. Ingham, A. Aggeli, N. Boden, T. A. Waigh and J. Fisher, *J. Biomed. Mater. Res., Part A*, 2006, **78**, 236–246.
37 S. Sankar, K. O'Neill, M. Bagot D'Arc, F. Rebeca, M. Buffier, E. Aleksi, M. Fan, N. Matsuda, E. S. Gil and L. Spirio, *Front. Bioeng. Biotechnol.*, 2021, **9**, 679525.
38 R. Behrendt, P. White and J. Offer, *J. Pept. Sci.*, 2016, **22**, 4–27.
39 R. Gambaretto, L. Tonin, C. Di Bello and M. Dettin, *Biopolymers*, 2008, **89**, 906–915.
40 R. V. Ulijn and A. M. Smith, *Chem. Soc. Rev.*, 2008, **37**, 664.
41 Y. Loo, S. Zhang and C. A. E. Hauser, *Biotechnol. Adv.*, 2012, **30**, 593–603.
42 G. Lippens, J.-M. Wieruszeski, A. Leroy, C. Smet, A. Sillen, L. Buée and I. Landrieu, *ChemBioChem*, 2004, **5**, 73–78.